γH2AX and cleaved PARP-1 as apoptotic markers in irradiated breast cancer BT474 cellular spheroids

O.F. QVARNSTRÖM[1], M. SIMONSSON[1], V. ERIKSSON[2], I. TURESSON[1] and J. CARLSSON[2]

Sections of [1]Oncology and [2]Biomedical Radiation Sciences, Department of Oncology, Radiology and Clinical Immunology, Rudbeck Laboratory, Uppsala University, SE-751 85 Uppsala, Sweden

Received January 15, 2009; Accepted March 19, 2009

DOI: 10.3892/ijo_00000311

Abstract. Chemo- and radiotherapy induce apoptosis in tumours and surrounding tissues. In a search for robust and reliable apoptosis markers, we have evaluated immunostaining patterns of γH2AX and cleaved PARP-1 in paraffin-embedded cellular spheroids. Breast cancer BT474 cells were grown as cell spheroids to diameters of 700-800 μm. The spheroids contained an outer cell layer with proliferative cells, a deeper region with quiescent cells and a central area with necrosis. They were irradiated with 5 Gy and the frequency of apoptotic cells was determined at several time points (0-144 h) and distances (0-150 μm) from the spheroids surface. γH2AX and cleaved PARP-1 were quantified independently. Apoptotic frequencies for the two markers agreed both temporally and spatially in the proliferative regions of the spheroids. The γH2AX signal was stronger and had lower background compared to cleaved PARP-1. The central necrotic region was intensely stained with cleaved PARP-1, whereas no γH2AX could be detected. The apoptotic frequency increased with distance from surface for all time points. However, apoptotic frequencies, above unirradiated control levels, could only be detected for the last time point, 144 h after irradiation. We have shown that the spheroid model is a practical system for evaluation of staining patterns and specificities of apoptosis markers. Also, the radial gradient provides the opportunity to study apoptosis under a range of physiological conditions within the same system. We have further shown that γH2AX and cleaved PARP-1 are applicable markers for apoptosis in the proliferative regions of the spheroids. However, the more intense and clear staining patterns of γH2AX suggests that this marker is preferable for quantification of apoptosis in spheroids and similar paraffin-embedded materials.

Correspondence to: Fredrik Qvarnström, Section of Oncology, Department of Oncology, Radiology and Clinical Immunology, Rudbeck Laboratory, Uppsala University, SE-751 85 Uppsala, Sweden
E-mail: qvasim@qvasim.com

Key words: apoptosis, breast cancer cells, BT474, cell spheroids, γH2AX, PARP, radiation effects

Introduction

Apoptosis induced by chemo- and radiotherapy has been extensively studied in a wide range of tumour cells (1-10). Analysis of radiation-induced apoptosis is of interest for studies of death effects due to the daily radiation doses of ~2 Gy that most often is given in conventional radiation therapy (11,12) and also after therapy with radionuclides with low dose rate (13-15).

A wide range of methods and markers are currently available for detection and quantification of apoptosis. In this study we evaluate a method for apoptosis quantification which involves γH2AX, a surrogate marker for DSBs. Apoptosis-related DNA fragmentation can result in massive induction of DSBs, which in turn has been shown to induce H2AX phosphorylation (16). This suggests that γH2AX, besides its DSB detecting abilities, also could serve as a marker for apoptosis (17). The apoptotic specificity has since then been validated in several studies where γH2AX has been compared with other apoptotic markers and apoptotic cellular morphology (18-20).

We have further compared the γH2AX apoptotic staining pattern by double-staining with cleaved PARP-1, a commonly used and well-established apoptotic marker (18,20,21). PARP-1 is cleaved *in vivo* by Caspase-3 and is suggested to be an apoptotic-specific event, aimed at stopping the highly energy consuming PARP-1 activity and thereby avoiding energy depletion and uncontrolled cell death by necrosis (21-24).

We have evaluated these apoptotic markers in paraffin-embedded cellular spheroids which mimic the properties of *in vivo* tumour nodules. The structure of a tumour nodule can be described as a three-dimensional nodular pattern. Proliferative cells reside near the blood vessels and capillaries. At some distance from these, the quiescent cells are located. Necrotic areas are formed even further away, i.e. 150-300 μm, from the nearest blood vessel or capillary (25-27). Apoptosis is expected to be found within the layers of viable cells.

Many of the unwanted variations affecting *in vivo* studies (i.e. drug clearance, variations in nutrition supply, host defence mechanisms) can be avoided or at least minimized using the spheroid *in vitro* model (28). The advantage of the spheroid model is that it offers possibilities to study the action of therapy effective substances under strictly controlled conditions. The

spheroids share several structural features with tumour nodules. The spheroids are spherically shaped with an outer proliferative cell layer, an inner layer of mainly quiescent cells and a central core consisting of necrosis (15,29-32). It has been reported that there can be both necrosis and apoptosis in spheroids (31,33,34). The central necrosis area most often contain an amorphous degenerative mass or a more or less homogeneous assembly of pycnotic cells while apoptosis can be seen in the surrounding cell layers. The spheroid model has been established for tumour biological studies that focus on properties of micrometastases.

The spheroids have radial gradients regarding pH, pO_2, nutrition supply and catabolic products similar to those found in a metastatic tumour nodule *in vivo* (35). These gradients allow us to explore if γH2AX and cleaved PARP-1 (cPARP-1) respond differently under these conditions resulting in different staining patterns. Furthermore, the spheroid layout can provide information about differences in how apoptosis is induced in the outer proliferative cell layer in comparison to the inner quiescent cell layer of the spheroids. The markers specificity for apoptosis can also be evaluated since necrosis and apoptosis are confined to separate compartments of the spheroid.

In this study, we have investigated radiation-induced apoptosis in BT474 breast cancer cell spheroids by comparing the temporal and spatial staining patterns of the γH2AX and cPARP-1 apoptotic markers.

Materials and methods

Cell culture. The breast cancer BT474 cells (American Type Culture Collection, Manassas, VA) were grown as both monolayer cultures and cell spheroids in Ham's F10 cell culture medium (Biochrome KG, Berlin, Germany). All media were supplemented with 10% fetal bovine serum, L-glutamine (2 mM) and PEST (100 IU/ml penicillin, 100 μg/ml streptomycin), all from Biochrome KG. This culture medium is in the following called the complete medium. All cells were cultured at 37˚C in an incubator with humidified environment with 5% CO_2. The cells were trypsinized with trypsin-EDTA (0.25% trypsin, 0.02% EDTA in phosphate-buffered saline (PBS) without Ca and Mg, from Biochrome KG.

Growth of the spheroids. Monolayer cultures of BT474 cells were trypsinized for 10 min at 37˚C and the cell suspension was then diluted in complete culture medium and seeded in spinner flask cultures. The spinner flasks were of two types; big and small. The big spinners rotated around a horizontal axis, with a speed of ~50 rpm and contained 125 ml complete culture medium. Hundreds of spheroids formed spontaneously and started to grow in these big spinners. Smaller samples of ~10 spheroids could at any occasion be taken out and grown in smaller spinner flasks containing only 5 ml complete medium. These small spinners rotated around a horizontal axis, with a speed of ~20 rpm. All spinner cultures were grown at 37˚C in an incubator with humidified environment with 5% CO_2. To evaluate the normal growth rate of the spheroids, samples with ~10 spheroids in 5 ml medium were taken out daily and were fixed in formalin (4% formaldehyde in phosphate buffer solution, Solveco, Taby, Sweden). The diameter of these spheroids was measured using an ocular scale, in the eyepiece of an inverted microscope. Their volume was calculated with the relation $V = 4/3 \times \pi \times (a \times b)^{3/2}$ where a and b were radii measured at right angles by means of an ocular scale, in the eyepiece of an inverted microscope (Leica DMIL, Göteborg, Sweden).

Irradiation. When the spheroids had reached the size of 700-800 μm, 10 living spheroids were taken out from the spinner flasks and transferred to culture flasks containing 10 ml complete medium and were then immediately irradiated. The spheroids were irradiated, at 37˚C, with 5 Gy in a γ radiation apparatus (Gammacell 40 Exactor, MDS Nordion, Canada). The apparatus contains two ^{137}Cs sources each with the strength 66.5 TBq, 2001.

The dose rate during the spheroid irradiations was 1.16 Gy/min. Thereafter the 10 irradiated spheroids were transferred to small spinner flasks containing only 5 ml complete culture medium. They were thereafter grown for 24, 48 or 144 h before fixation. The culture medium was, in this case, changed every day.

Fixation and sectioning. Spheroids were fixed in formalin for 20 h, dehydrated in a graded alcohol scale (from 70 to 100%), infiltrated in xylene and paraffin using a VIP (Vacuum infiltrating processor, Ventana Renaissance, Ventana Medical Systems, Tucson, AZ), embedded in paraffin and sectioned to a thickness of ~5 μm per section. Totally 74 spheroids were individually analyzed. Central sections (with spheroids of maximal diameter) were selected for further analysis. The sections were then deparaffinized in xylene, washed in alcohol and processed further.

Staining with γH2AX, cPARP-1 and DAPI. A water bath (90˚C) was used for epitope retrieval. Sections were heated in a water bath for 40 min in boric acid buffer (pH 7.0). Immunohistochemical staining was performed with a mouse monoclonal antibody against γH2AX, dilution 1:100, (Upstate, Charlottesville, VA) and a rabbit monoclonal antibody against the p25 cleaved form of PARP-1 (Epitomics, Burlingame, CA). Alexa555 goat anti-mouse and Alexa488 goat anti-rabbit antibodies were used for secondary detection, dilution 1:100 (Molecular Probes, Eugene, OR). DAPI, 0.4 μg/ml (Molecular Probes) was used for nuclear staining. After antibody incubations, slides were washed for 3x5 min in PBS buffer (pH 7.4). Slides were mounted in Vectashield mounting medium (Vector Laboratories, Burlingame, CA). To account for possible variations in staining, spheroid stainings were performed at four separate occasions.

Image acquisition. Images of whole spheroids were acquired as 24-bit RGB images using a Spot Insight Colour CCD camera (Diagnostic Instruments, Sterling Heights, MI) attached to a fluorescence microscope, Nikon Eclipse E400, with a Nikon 10x objective. The cPARP-1, γH2AX and DAPI staining was recorded as an overlapping set meaning that, with the help of filters, each staining can be inspected and acquired separately in each section and, if interesting,

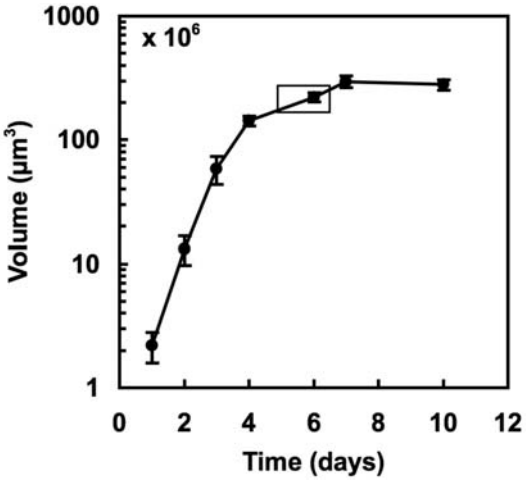

Figure 1. Growth of breast cancer BT474 spheroids in spinner flask culture. Measurements of at least 20 spheroids are presented as mean values with standard deviations. The square indicates the time and size when the spheroids were harvested.

afterwards summarized digitally. Totally 79 spheroid sections were evaluated.

Evaluation of the staining. The closest distance to the surface, for each apoptotic cell within the stained spheroids, was measured in the image analysis software imageJ. The surface distances of the apoptotic cells and the radii of the spheroids were further processed in the statistics software package R using a script that calculates the number of apoptotic cells per area. The areas were grouped so that the number of apoptotic cells was given in areas stepwise 50 μm from the surface towards the border of the necrotic area. The number of spheroids evaluated was 11 controls, 21 spheroids 24 h after irradiation, 31 spheroids 44 h after irradiation and 11 spheroids 144 h after irradiation. The reason for the large number of analyzed spheroids 24 and 44 h after irradiation was that several reproducibility stainings were made at these times. Since the reproducibility was good, all values were included in the final calculations of all measurements.

Basic characterization of the spheroids; ^{3}H-TdR-labeling index and cell density. Non-irradiated BT474 spheroids with diameter 700-800 μm were labelled with ^{3}H-TdR with a specific radioactivity of 5 Ci/mmol (Radiochemical Centre, Amersham, London, UK). Culture medium with 37 kBq/ml was added to the cell spheroids for 24 h, with the spheroids grown in the small spinner flasks, as described above. Thereafter the spheroids were washed in complete medium without radioactivity and then fixed, embedded in paraffin and sectioned as described above. The sections were processed for autoradiography by the dipping technique using K5 emulsion (Ilford Scientific, London, UK) and left in the dark for 28 days before development in Kodak D19 and fixation with UNIFIX (Kodak, Rochester, USA). The sections were then stained with haematoxylin. The numbers of both labelled and unlabelled cells were counted in a square, covering 50x50 μm of the spheroid sections, mounted in the eyepiece of a Leitz Ortholux microscope, Wetzlar, Germany.

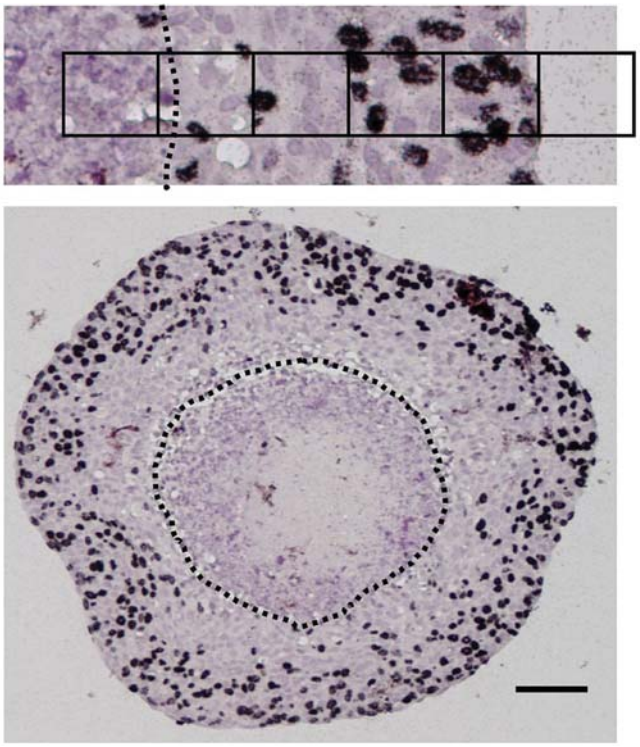

Figure 2. Morphological appearance of a BT474 spheroid (diameter = 800 μm and sectioned in 5 μm slices) processed for autoradiography after 24 h incubation with ^{3}H-TdR. The dark spots show labelled cell nuclei. The dotted lines indicate the border to central necrosis. The upper panel shows a grid with 50x50 μm squares that were applied to count the number of cells and the fraction of labelled cell nuclei as a function of depth in the spheroids. The lower panel shows an overview of the whole spheroid. The bar in lower right corner corresponds to 100 μm.

The evaluation proceeded stepwise along the radius, from the surface of the spheroids into the necrosis area, with a distance of 50 μm per step. The 40x objective was used during the evaluation. Six radii from each of 7 spheroids (diameters 700-800 μm) were analyzed, thus totally 42 radii were evaluated.

Results

Growth of breast cancer BT474 spheroids. The volume growth of breast cancer BT474 spheroids in spinner flask culture is shown in Fig. 1. The morphological appearance of a typical BT474 spheroid labelled with ^{3}H-TdR is shown in Fig. 2. The proliferation gradient, measured as the gradient in fraction of ^{3}H-TdR labelled cell nuclei and the cell density gradient were quantitatively evaluated (Fig. 3). The cell density was constant in the outer layers of the spheroids while the density decreased in the deeper regions. There were no proliferative cells in the deeper regions close to the central necrosis.

γH2AX and cPARP-1 co-localise with apoptotic cells. Sections of BT474 spheroids were simultaneously stained with γH2AX, cPARP-1 and DAPI (Fig. 4). Co-localisation between γH2AX and cPARP-1 confirms the apoptotic status of the intensely γH2AX-stained cells (Fig. 4d). The nuclear DAPI staining further revealed that a subset of γH2AX-stained apoptotic cells also displayed several morphological features of apoptosis such as nuclear condensation, rounding and formation of

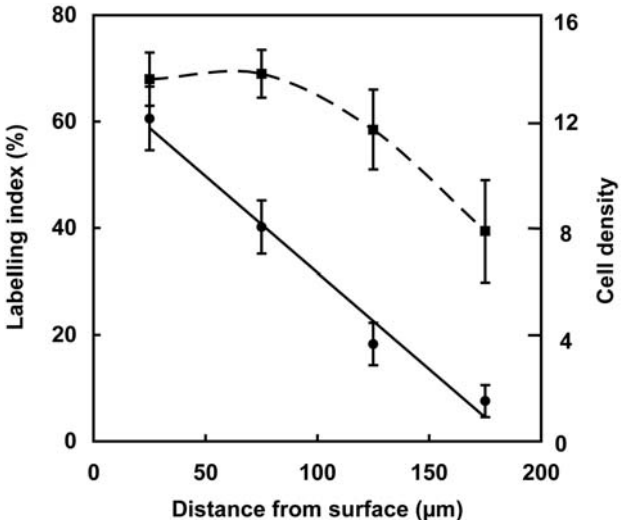

Figure 3. ^{3}H-TdR labelling index and cell density in 50x50 μm squares as a function of depth in control BT474 breast cancer spheroids. The filled circles and solid line represents labelling indices and the filled squares and dotted line represents cell density. Evaluations of 42 radii are presented as mean values with standard deviations.

apoptotic bodies. The γH2AX apoptotic staining pattern was easily distinguished from previously described foci patterns corresponding to individual DSBs (16,36).

At the latest time point investigated, 144 h after irradiation, the frequency of apoptotic cells had increased 2-3 times compared to unirradiated controls. Examples of γH2AX and cPARP-1 staining at this time point are shown in Fig. 5. The γH2AX staining was stronger and had better contrast compared to cPARP-1 and some γH2AX-positive cells could not be detected with cPARP-1. Various stages of nuclear fragmentation could be seen in both γH2AX and cPARP-1-positive cells. The fragmentation was, however, more apparent in the γH2AX staining due to the stronger signal (Fig. 5).

At all time points investigated the central necrotic region was intensely stained with cPARP-1, whereas no γH2AX could be detected in this region.

γH2AX and cPARP-1 increase with time and depth in the proliferative region. The spheroids have radial gradients regarding pH, pO_2, nutrition supply and catabolic products similar to those found in a metastatic tumour nodule *in vivo*. To investigate if these gradients had an impact on expression of γH2AX and cPARP-1, the spheroid sections were analysed in three concentric annular segments in steps of 50 μm from the outside towards the central necrotic region. Spheroids were scored for γH2AX and cPARP-1-stained cells with a distance to the spheroid surface of 0-50 μm (Fig. 6a), 50-100 μm (Fig. 6b) and 100-150 μm (Fig. 6c). The time zero corresponds to values for the un-irradiated control spheroids.

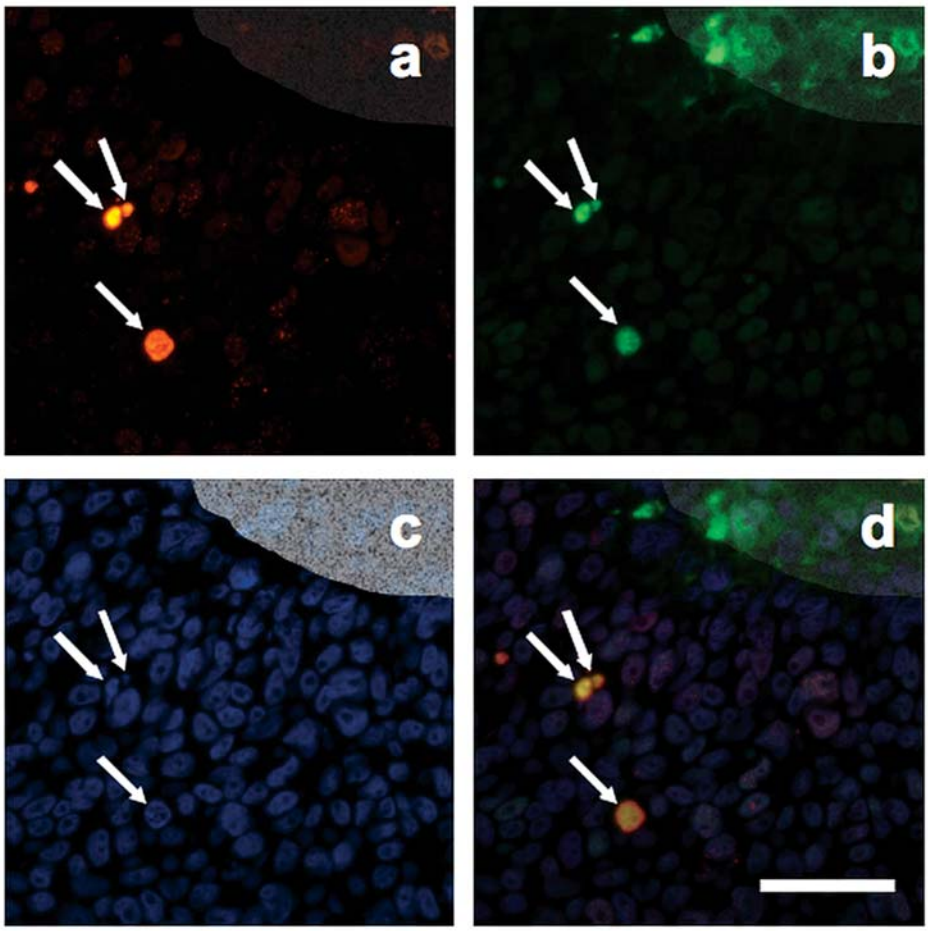

Figure 4. Example of a γH2AX (a), cPARP-1 (b) and DAPI (c) immunofluorescence stainings in a section of a BT474 spheroid, 44 h after irradiation. (d) An overlay of (a-c). The arrows indicate three apoptotic cells, where γH2AX and cPARP-1 stainings co-localise. The shaded areas in the upper right corners mark the central necrotic region. Note that the central necrotic region is cPARP-1-positive and γH2AX-negative. The bar corresponds to 50 μm.

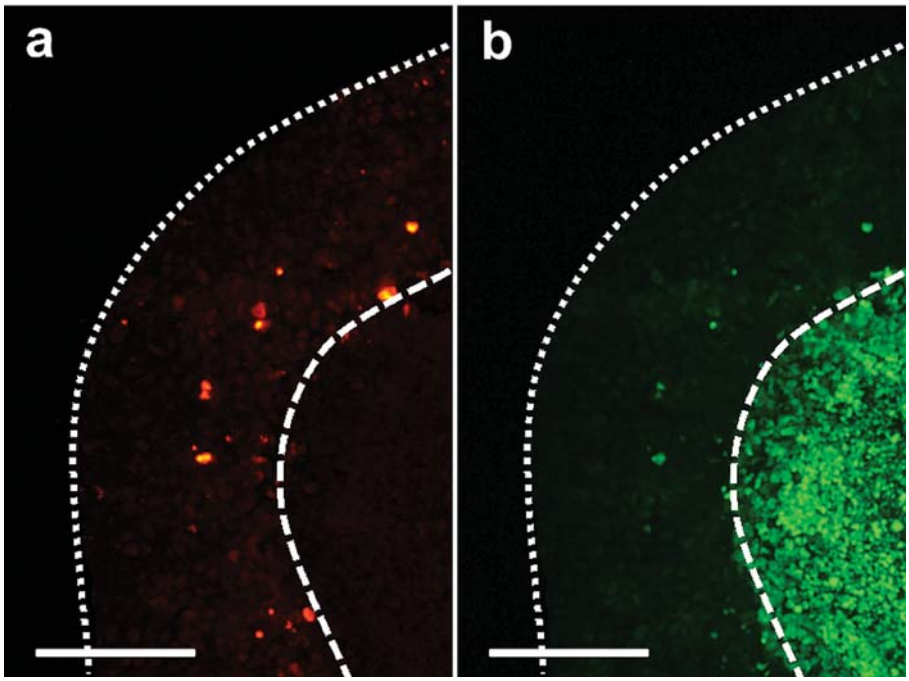

Figure 5. Example of a γH2AX (a) and cPARP-1 (b) immunofluorescence stainings in a section of a BT474 spheroid, 144 h after irradiation. The dotted line indicates the outer surface of the spheroid and the dashed line indicate the border to necrosis. Note that the central necrotic region is cPARP-1-positive and γH2AX-negative. The bars correspond to 100 μm.

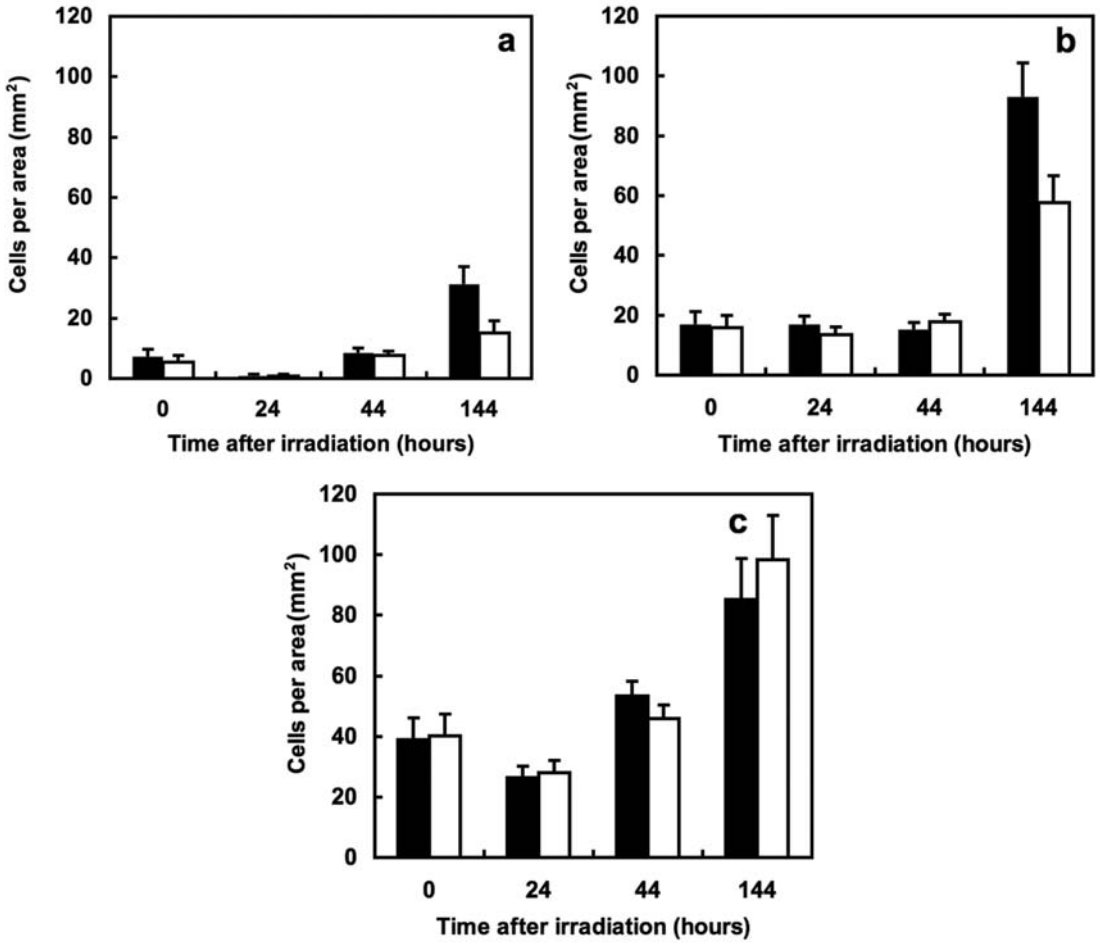

Figure 6. Quantitative evaluations of the frequency of γH2AX (filled bars) and cPARP-1 (open bars)-stained cells at increasing distances from the spheroid surface at three time points after 5 Gy irradiation. The time zero corresponds to values for the non-irradiated controls. The three plots display the apoptotic frequencies at different depths in the spheroids; (a) 0-50 μm, (b) 50-100 μm and (c) 100-150 μm. Data are presented as mean values and standard deviations. Apoptotic frequency is presented as cells per mm^2.

The γH2AX and cPARP-1 staining patterns exhibit conformity both temporally and spatially in the proliferative regions of the spheroids. For both markers an increase in apoptotic frequency could only be detected for the latest time point 144 h after irradiation. Also, the apoptotic frequency increased with distance to surface for all time points.

Discussion

Evaluation of molecular markers using cellular spheroids. There are currently a wide range of markers and methods available for apoptosis detection in cells and tissues. Cellular spheroids offer a well-controlled and reproducible system for comparing and testing these markers under conditions that resembles those found in micro metastases *in vivo*.

γH2AX specificity for apoptosis. The reported temporal and spatial co-localisation for γH2AX with cPARP-1 as well as morphological features seen in DAPI support previous observations that γH2AX is a reliable marker for apoptosis (18-20). Furthermore, the signal from massive DNA fragmentation detected with γH2AX is very strong compared to cPARP-1. This allows for more robust and sensitive detection when quantifying apoptosis.

Other types of cell death, such as necrosis, also involve DNA fragmentation and could potentially cause ambiguous results when DNA fragmentation is used as a basis for apoptosis detection. Even though necrotic DNA fragmentation is random, late, and predominantly consisting of single-strand breaks, methods like the TUNEL assay, which detects the ends of broken DNA strand, also have an ability to detect necrosis to various degrees (22,37). Interestingly, no γH2AX staining was observed in the central necrotic region of the spheroids.

The central necrotic region was, however, intensely stained with cPARP-1. This staining pattern is surprising since cleavage of PARP-1 generally is suggested to be an apoptotic-specific event, aimed at stopping the highly energy-consuming PARP-1 activity and thereby avoiding energy depletion and uncontrolled cell death by necrosis (21-24).

From this perspective, considering higher sensitivity and higher specificity, the use of γH2AX for apoptosis detection in spheroids and similar materials should be preferred over cPARP-1.

Comparison of γH2AX and cPARP-1 as apoptotic markers. There was a tendency for higher apoptotic frequency when scoring γH2AX compared to cPARP-1 in the material. This was possibly due to the higher sensitivity of γH2AX resulting in more apoptotic cells being detected. The stronger signal also had an impact on the scoring of cells with fragmented nuclei. With more fragments being detected it could sometimes be difficult to conclude if the fragments belonged to one or more cells. This effect was more pronounced for later time points and deeper regions with many apoptotic cells in close vicinity. Differences in detection levels could also occur if the two markers detected slightly different stages of apoptosis. However, as determined by morphological observations, both markers were able to detect both early and late events in the apoptotic pathway.

The scoring should not be affected by the differences in staining patterns for γH2AX and cPARP-1 in necrotic cells, since the quantification of apoptosis was limited to the outer 150 μm of the spheroids.

The error bars presented in Fig. 6 is based on Poisson distribution for the apoptotic events. However, these error bars do not accommodate for all of the variations in the experimental setup. There are probably slight variations between sections from the same spheroid and between spheroids as well as between different stainings. Furthermore, there is a difference in sampling since the number of spheroids available for different time points differed and depending on the geometry of spheroids, more area was analysed for distances close to the surface. The uncertainty due to fragmented nuclei was also more pronounced for later time points and deeper regions. However, determining the exact magnitude is beyond the scope of this study, since the conclusions drawn are focused on the comparison of γH2AX and cPARP-1 as apoptotic markers.

Apoptosis as a function of time and depth in the spheroids. A general increase in apoptotic frequency could only be recorded for the latest time point, 6 days after damage induction. The data therefore suggest that radiation-induced apoptosis in the spheroids occurs relatively late and that the onset is more sudden than continuous.

All time points revealed a continuous increase in apoptotic frequencies with distance to spheroid surface. Also, comparisons of the different time points reveal that the increase in apoptosis is slightly more pronounced for the outer regions (see Fig. 6). For instance, at the 144 h time point, γH2AX determined apoptosis has increased by 4 times for the outer zone (0-50 μm) and only 2 times for the inner zone (100-150 μm). Since apoptosis can be a stress induced event, it is likely that the observed apoptotic gradient is a direct reflection of the increasingly toxic environment towards the inner regions of the spheroid.

It is noteworthy that the increase in apoptotic frequency due to the toxic environment close to the central region is comparable to the one seen after 5 Gy at the latest time point in the outer regions.

Quantification of DSB-related γH2AX foci and apoptosis. γH2AX is commonly used as a surrogate marker for DSBs, visualising the breaks as bright foci in the cell nuclei. The opportunity to simultaneously detect and quantify apoptosis and radiation induced foci in the same sample could, however, not be explored since the time points chosen for apoptosis were unsuitable for foci detection. At our earliest time point, 24 h following radiation, most of the initial DSB-induced foci are expected to be repaired.

Furthermore, reliable quantification of DSBs requires detecting and counting of individual foci. The dose of 5 Gy, chosen to induce sufficient levels of apoptosis, is not optimal since this will result in a high degree of foci overlap (36,38).

In conclusion, the described approach for measuring apoptosis as a function of depth in spheroids has several interesting implications. It provides a versatile tool for evaluation of molecular markers that in turn can be applied to

studies on several types of anti-cancer drugs and treatments. γH2AX proved to be a robust and distinct marker for apoptosis in formalin-fixed, paraffin-embedded spheroids.

Acknowledgements

The study was financially supported by a grant from the Swedish Cancer Society (0980-B07-20XCC, contract no.: 070070).

References

1. Olive PL and Durand RE: Apoptosis: an indicator of radiosensitivity in vitro? Int J Radiat Biol 71: 695-707, 1997.
2. Verheij M and Bartelink H: Radiation-induced apoptosis. Cell Tissue Res 301: 133-142, 2000.
3. Shinomiya N: New concepts in radiation-induced apoptosis: 'premitotic apoptosis' and 'postmitotic apoptosis'. J Cell Mol Med 5: 240-253, 2001.
4. Mirzaie-Joniani H, Eriksson D, Johansson A, Lofroth PO, Johansson L, Ahlstrom KR and Stigbrand T: Apoptosis in HeLa Hep2 cells is induced by low-dose, low-dose-rate radiation. Radiat Res 158: 634-640, 2002.
5. Mirzaie-Joniani H, Eriksson D, Sheikholvaezin A, Johansson A, Lofroth PO, Johansson L and Stigbrand T: Apoptosis induced by low-dose and low-dose-rate radiation. Cancer 94: 1210-1214, 2002.
6. Norbury CJ and Zhivotovsky B: DNA damage-induced apoptosis. Oncogene 23: 2797-2808, 2004.
7. Brown JM and Attardi LD: The role of apoptosis in cancer development and treatment response. Nat Rev 5: 231-237, 2005.
8. Viktorsson K, Lewensohn R and Zhivotovsky B: Apoptotic pathways and therapy resistance in human malignancies. Adv Cancer Res 94: 143-196, 2005.
9. Golstein P and Kroemer G: A multiplicity of cell death pathways. Symposium on apoptotic and non-apoptotic cell death pathways. EMBO Rep 8: 829-833, 2007.
10. Galluzzi L, Maiuri MC, Vitale I, Zischka H, Castedo M, Zitvogel L and Kroemer G: Cell death modalities: classification and pathophysiological implications. Cell Death Differ 14: 1237-1243, 2007.
11. Steel GG: Basic Clinical Radiobiology. Arnold Publisher and Hodder Headline Group, London, 2002.
12. Hall EJ and Giaccia AJ: Radiobiology For The Radiologist. Chapter 5. Lippincott Williams & Wilkins, Philadelphia, 2006.
13. Carlsson J, Håkansson E, Eriksson V, Grawe J, Wester K, Grusell E, Montelius A and Lundqvist H: Early effects of low dose-rate radiation on cultured tumor cells. Cancer Biother Radiopharm 18: 663-670, 2003.
14. Carlsson J, Eriksson V, Stenerlöw B and Lundqvist H: Requirements regarding dose rate and exposure time for killing of tumour cells in beta particle radionuclide therapy. Eur J Nucl Med Mol Imaging 33: 1185-1195, 2006.
15. Carlsson J and Gedda L: Penetration of tumor therapy interesting substances in non-vasularized metastases: review of studies in multicellular spheroids. Curr Cancer Ther Rev 2: 293-304, 2006.
16. Rogakou EP, Pilch DR, Orr AH, Ivanova VS and Bonner WM: DNA double-stranded breaks induce histone H2AX phosphorylation on serine 139. J Biol Chem 273: 5858-5868, 1998.
17. Rogakou EP, Nieves-Neira W, Boon C, Pommier Y and Bonner WM: Initiation of DNA fragmentation during apoptosis induces phosphorylation of H2AX histone at serine 139. J Biol Chem 275: 9390-9395, 2000.
18. Holubec H, Payne CM, Bernstein H, Dvorakova K, Bernstein C, Waltmire CN, Warneke JA and Garewal H: Assessment of apoptosis by immunohistochemical markers compared to cellular morphology in ex vivo-stressed colonic mucosa. J Histochem Cytochem 53: 229-235, 2005.
19. Mukherjee B, Kessinger C, Kobayashi J, Chen BP, Chen DJ, Chatterjee A and Burma S: DNA-PK phosphorylates histone H2AX during apoptotic DNA fragmentation in mammalian cells. DNA Repair 5: 575-590, 2006.
20. Simonsson M, Qvarnstrom F, Nyman J, Johansson K, Garmo H and Turesson I: Low-dose hypersensitive gammaH2AX response and infrequent apoptosis in epidermis from radiotherapy patients. Radiother Oncol 88: 388-397, 2008.
21. Koh DW, Dawson TM and Dawson VL: Mediation of cell death by poly(ADP-ribose) polymerase-1. Pharmacol Res 52: 5-14, 2005.
22. Stadelmann C and Lassmann H. Detection of apoptosis in tissue sections. Cell Tissue Res: 301: 319-331, 2000.
23. Bouchard VJ, Rouleau M and Poirier GG: PARP-1, a determinant of cell survival in response to DNA damage. Exp Hematol 31: 446-454, 2003.
24. D'Amours D, Sallmann F, Dixit V and Poirier G: Gain-of-function of poly(ADP-ribose) polymerase-1 upon cleavage by apoptotic proteases: implications for apoptosis. J Cell Sci 114: 3771-3778, 2001.
25. Thomlinson RH and Gray LH: The histological structure of some human lung cancers and the possible implications for radiotherapy. Br J Cancer 9: 539-549, 1955.
26. Tannock IF: The relation between cell proliferation and the vascular system in a transplanted mouse mammary tumour. Br J Cancer 22: 258-273, 1968.
27. Mayr NA, Staples JJ, Robinson RA, Vanmetre JE and Hussey DH: Morphometric studies in intraductal breast carcinoma using computerized image analysis. Cancer 67: 2805-2812, 1991.
28. Fracasso G and Colombatti M: Effect of therapeutic macromolecules in spheroids. Crit Rev Oncol Hematol 36: 159-178, 2000.
29. Sutherland RM and Durand RE: Radiation response of multicell spheroids - an in vitro tumour model. Curr Top Radiat Res Q 11: 87-139, 1976.
30. Carlsson J and Yuhas JM: Liquid-overlay culture of cellular spheroids. Recent Results Cancer Res 95: 1-23, 1984.
31. Mueller-Klieser W: Multicellular spheroids. A review on cellular aggregates in cancer research. J Cancer Res Clin Oncol 113: 101-122, 1987.
32. Sutherland RM: Cell and environment interactions in tumor microregions: the multicell spheroid model. Science 240: 177-184, 1988.
33. Santini MT, Rainaldi G and Indovina PL: Apoptosis, cell adhesion and the extracellular matrix in the three-dimensional growth of multicellular tumor spheroids. Crit Rev Oncol Hematol 36: 75-87, 2000.
34. Indovina P, Rainaldi G and Santini MT: Three-dimensional cell organization leads to a different type of ionizing radiation-induced cell death: MG-63 monolayer cells undergo mitotic catastrophe while spheroids die of apoptosis. Int J Oncol 31: 1473-1483, 2007.
35. Carlsson J and Acker H: Relations between pH, oxygen partial pressure and growth in cultured cell spheroids. Int J Cancer 42: 715-720, 1988.
36. Qvarnström OF, Simonsson M, Johansson KA, Nyman J and Turesson I: DNA double strand break quantification in skin biopsies. Radiother Oncol 72: 311-317, 2004.
37. Grasl-Kraupp B, Ruttkay-Nedecky B, Koudelka H, Bukowska K, Bursch W and Schulte-Hermann R: In situ detection of fragmented DNA (tunel assay) fails to discriminate among apoptosis, necrosis, and autolytic cell death: A cautionary note. Hepatology 21: 1465-1468, 1995.
38. Böcker W and Iliakis G: Computational Methods for analysis of foci: validation for radiation-induced gamma-H2AX foci in human cells. Radiat Res 165: 113-124, 2006.